Cold Regions Science and Technology 90–91 (2013) 38–52

Contents lists available at SciVerse ScienceDirect

Cold Regions Science and Technology

journal homepage: www.elsevier.com/locate/coldregions

Monitoring and modeling the influence of snow pack and organic soil on a permafrost active layer, Qinghai–Tibetan Plateau of China

Jian Zhou [a,*], Wolfgang Kinzelbach [b], Guodong Cheng [a], Wei Zhang [c], Xiaobo He [a], Bosheng Ye [a]

[a] State Key Laboratory of Frozen Soil Engineering, Cold and Arid Regions Environmental and Engineering Research Institute, Chinese Academy of Sciences, Lanzhou 730000, China
[b] Institute of Environmental Engineering, ETH Zurich, Wolfgang-Pauli-Strasse 15, 8093 Zurich, Switzerland
[c] Resources and Environment Institute, Lanzhou University, Lanzhou 730000, China

ARTICLE INFO

Article history:
Received 31 May 2012
Accepted 12 March 2013

Keywords:
Qinghai–Tibetan Plateau
Active layer
Organic soil
Snow pack
CoupModel

ABSTRACT

As a result of global warming, the depth of the permafrost active layer on the Qinghai–Tibet Plateau (QTP) has been increasing progressively during the past few decades. The Cold and Arid Regions Environmental and Engineering Research Institute, Chinese Academy of Sciences, established the Binggou and Tanggula research stations on the QTP to monitor the impacts of snow pack and tundra soil on the permafrost active layer. In order to reproduce active layer dynamics in the present climate, the CoupModel, which calculates vertical heat and water processes in a soil–snow–atmosphere system, was successfully adjusted and applied for the two research stations. Subsequently, the calibrated model was used to provide an evaluation of the potential response of the active layer to different scenarios of climate warming and precipitation increase at Binggou station. The results reveal: ① the soil freezes deeper for snow depths less than 20 cm in the present climate, compared to the situation without snow cover. Increased albedo, due to shallow snow cover, reduces the absorption of solar irradiation and decreases soil temperature. However, this positive effect is lost with increasing precipitation and snow depth in winter. The decrease of simulated cumulative ground heat flux in winter along with thicker snow depth indicates that the thicker snow pack gradually insulates the subsoil against energy losses to the atmosphere in winter, which induces a reduction of active layer frozen depth. ② The model predicted an increase of maximum active layer thawing depth from today 150 cm to about 350 cm as a result of a 4 °C warming and a talik formation at the top of the permafrost as a result of a 6 °C warming. The other investigation concerns the influence of organic soil layer depth on the active layer at Tanggula station. The model results reveal that the maximum thawing depth of the active layer in summer gradually decreases along with the increase of the soil organic layer depth. The maximum thawing depth is close to 300 cm when ignoring the organic layer, while it is about 150 cm with a realistic organic layer of 40 cm depth. The results reveal that the organic layer provides a protection against active layer deepening in summer. Therefore, both the roles of snow and organic soil are of importance for the behavior of permafrost under climate warming conditions.

1. Introduction

The active layer is the layer of soil or other earth materials between the atmosphere and the permafrost body. It is subject to freezing and thawing on an annual basis and responsible for most of the exchange of energy, moisture, and gasses between atmosphere and subsurface (Kane et al., 1991; Nelson and Anisimov, 1993; Zhang, 2005). Globally, an area of about 50×10^6 km^2 of surface soil undergoes freeze/thaw cycles annually (Kimball et al., 2001; Zhang et al., 2003b). The soil freeze/thaw status of the active layer has a profound influence on the energy and water exchange between the land surface and the atmosphere, the hydrological cycle, biological processes, and the carbon cycle (Goodison et al., 1998; Hinzman et al., 2003; Kane et al., 1991; Nelson et al., 1993; Weller et al., 1995; Zhang and Armstrong, 2001).

Increase of the active layer depth and degeneration of permafrost are important indicators of a warming climate. The increasing active layer thickness is an immediate indicator of warming, while the retreat of permafrost requires much longer times (Goodison et al., 1998; Li et al., 2008; Zhang et al., 2003a). There is an increasing belief that substantial changes in the active layer thickness may take place in the next few decades (Anisimov et al., 1997; Lawrence and Slater, 2005; Stendel and Christensen, 2002). Warmer climate generally results in a deeper active layer, but in some regions it produces the opposite effect. For example, the active layer decreased slightly in the last 30 years at Barrow, Alaska (Osterkamp, 2007) and parts of north-western Canada (Allison et al., 2001), although annual air temperature increased. The researchers explained that the decreasing snow depth allowed additional cooling of the ground in winter, which may not be compensated by summer warming (Allison et al.,

* Corresponding author. Tel.: +86 13919780625.
E-mail addresses: zhoujian@lzb.ac.cn (J. Zhou), kinzelbach@ifu.baug.ethz.ch (W. Kinzelbach), gdcheng@lzb.ac.cn (G. Cheng), yebs@lzb.ac.cn (W. Zhang), zw_2010@lzu.edu.cn (X. He), hxb@lzb.ac.cn (B. Ye).

0165-232X/$ – see front matter.
http://dx.doi.org/10.1016/j.coldregions.2013.03.003

2001). Meanwhile, warmer climatic conditions may result in the increase of organic content of soil layer, in which case the overall net effect would be a shallower active layer (Mölders and Romanovsky, 2006; Nicolsky et al., 2007). So, understanding the mechanisms of heat exchange between subsurface and near surface atmosphere is critical for predicting the response of the active layer to climatic change. One major obstacle for assessing changes in the soil thermal regime under climatic change is the lack of long-term observations of soil temperature and related climate variables (Zhang et al., 2001).

In the last 20 years, the response and feedback of the active layer to climatic change have received much attention in many international organizations and research projects. The Climate and Cryosphere (CliC) Project Science and Coordination Plan (http://ipo.npolar.no/reports/archive/wcrp_114.pdf) has declared the change of the active layer and of the distribution of permafrost as important research items in global warming research (Allison et al., 2001). The Coordinated Energy and Water Cycle Observation Project (CEOP, 2008) (http://www.ceop.net/) is strengthening the research into the influence of the soil freezing/thawing status on energy and water exchange between the land surface and the atmosphere in cold regions. As part of the Global Energy and Water Cycle Experiment (GEWEX) and the Coordinated Energy and Water Cycle Observation Project (CEOP), the GAME-Tibet Project (http://monsoon.t.u-tokyo.ac.jp/tibet/tibetmap.html) was initiated in 1997 by the Sino–Japanese monsoon cooperation group to clarify the energy and water cycles between the land surface and the atmosphere over the QTP in the context of the Asian monsoon system (Ma et al., 2003). Permafrost active layer and permafrost thermal state were identified as key cryospheric variables by the International Permafrost Association (IPA). As a result, the Global Terrestrial Network for Permafrost (GTNet-P), which was established under the Global Climate Observation System (GCOS) and the Global Terrestrial Observation System (GTOS) of the World Meteorological Organization (WMO), focuses on developing data sets of ground temperature, maximum thickness of the seasonal thawing, active layer characteristics and permafrost thermal state. Monitoring of active layer and borehole temperatures on the QTP is an important component of the Global Terrestrial Network for Permafrost (Brown et al., 2000).

With an average elevation of more than 4000 m, the QTP has one of the highest and largest permafrost areas in the Earth's mid- and lower latitudes, and is regarded as the third pole of the earth (Cheng, 1984). The changes of the plateau's cryospheric elements not only affect the regional climate, but also play an important role in the global processes (Cheng and Wu, 2007; Liu and Chen, 2000). The cryosphere on the QTP has unique characteristics. The QTP permafrost region is characterized by its unique semiarid climate (precipitation < 450 mm) and relatively little snowfall (Wang et al., 2009). Tundra soils, which are characterized by a surface organic layer of varying thickness and a wet mineral zone underlain by perennially frozen ground, are widely distributed on the QTP (Wang et al., 2008). Different from the arctic region, 50% of the permafrost region of the QTP belong to relatively warm permafrost, with annual mean ground temperatures usually between −0.5 °C and −1 °C and containing many taliks (Cheng, 2005; Wu, 2005). This warm permafrost is very sensitive to climate warming (Wu et al., 2007). Observed evidence shows that permafrost has been warming, thawing, and degrading during the past few decades on the QTP (Cheng and Wu, 2007; Wu and Zhang, 2008). Over the period 1995–2004, active layer thickness (ALT) has deepened by 10–40 cm in permafrost regions (Wu and Liu, 2004; Wu et al., 2006; Yang et al., 2004). Depth of seasonally frozen soil has decreased, on average, by 22 cm, at an average rate of 0.71 cm/yr since the 1980s over the eastern QTP (Wang et al., 2005; Zhao et al., 2004).

Many factors affect active-layer thickness and permafrost thermal state. Among the most important are air temperature, solar radiation, vegetation, soil moisture, duration and thickness of snow, the thermal properties of soil, and the near-surface organic layer (Brown et al., 2000; Frauenfeld et al., 2004; Zhang et al., 2005). Based on shallower snow depth and the extensive distribution of tundra soils on the QTP, two field stations (Binggou station and Tanggula station) were established by the Cold and Arid Regions Environmental and Engineering Research Institute, Chinese Academy Sciences (CAREERI, CAS) to observe the thermodynamic impact of snow and organic soil on the energy balance and thermal states within active layer. Predicting the soil frost conditions for the future may be made using mathematical modeling to reproduce current active layer dynamics and provide an estimate of the potential feedback of thawing permafrost layers and subsurface heat exchange between subsurface and atmosphere near surface in the future climate.

In this study, simulations were carried out using the one-dimensional heat and water flow model, CoupModel, based on weather conditions, snow depth, vegetation, as well as thermal and physical properties of soils. Model calibration used site specific measurement data. The calibrated model is used to predict and demonstrate the effect of increasing air temperature and precipitation on active layer thickness at Binggou station. The other investigation into the effect of organic soil on active layer thickness was conducted at Tanggula station by comparing modeled soil temperature profiles for organic soil layers of different depth. The goal of this study is to provide a detailed understanding of the active layer response to soil texture, snow depth and warming climate on the QTP through observation and modeling.

2. Materials and methods

2.1. The study sites

2.1.1. Binggou station

Binggou station (100°11′ E, 38°04′ N, altitude 4146.4 m a.s.l.), located in the Qilian Mountains at the northeast edge of the QTP (Fig. 1), was chosen to study the effect of snow pack and climatic warming on the active layer. Binggou station belongs to a seasonally snow-covered region. The majority of land is covered by alpine meadows. The mean depth of the seasonal snowpack is about 0.2 m, up to a maximum of 0.6 m. Snow redistribution is remarkable because of the interaction between blowing snow and complex terrain. There is more snowfall in spring and autumn than in winter. Snowfall occurs from October to April, and sets in again in October after a rainy season lasting from May to September. Mean air temperature was about −2.5 °C in the 2008 snow season, with a minimum of −29.6 °C, and a maximum of 19.9 °C.

An automatic climate observation system (ACOS) recorded air temperature, air pressure, humidity and wind speed at a height of 1.5 m above the ground surface (Fig. 2). The shortwave radiation and long-wave radiation (in both upward and downward directions) were also measured at 1.5 m above the ground surface (Fig. 2). Precipitation was recorded at one hour intervals. Soil temperature data were collected at depths of 0.1 m, 0.2 m, 0.4 m, 0.8 m and 1.2 m. Two heat flux meters were inserted at 0.02 m and 0.2 m depth. Soil samples were collected from the ground level to a depth of 1.2 m near the meteorological station. The samples were analyzed in the laboratory to determine soil bulk density, and composition in terms of sand, silt, clay, and organic matter content (Table 1). Snow data were collected through a series of field measurements in the snow season of 2008. Blowing snow was recorded with the FlowCapt Sensor (FlowCapt, Switzerland). The datasets include basic snow properties such as snow depth, density, grain size, temperature, and emissivity. Table 2 provides details of the main instruments used at this station.

2.1.2. Tanggula station

To quantify the influence of organic soil on the active layer on the QTP, a typical cryospheric station (Tanggula Cryospheric Station), located at the headwater of the Yangtze River in the center of the QTP (33°02′ N, 92°00′ E, altitude 5140 m a.s.l.), was selected as the

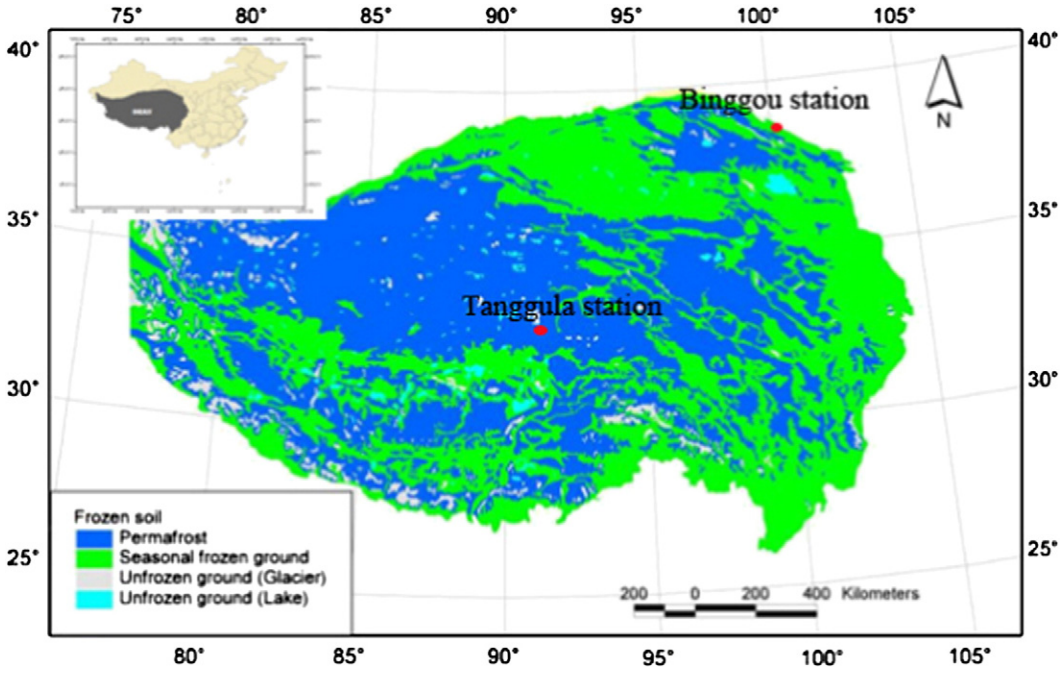

Fig. 1. Location of Binggou and Tanggula stations.

study site (Fig. 1). The Qinghai–Tibet highway passing through Tanggula Mountain Pass makes a long-term observation possible. A surface organic layer (0.20–1 m depth) is frequently present in the region. During the summer melting season, the basin is under the influence of the Indian monsoon, and the weather is rainy, wet and warm. In the winter season (from October to the following May), the basin is under the influence of the Westerly Circulation, with sunny, windy, dry and cold weather (Zhang et al., 1997). The annual average temperature is −6.0 °C, and the average annual precipitation is about 662 mm. The annual temperature range is 24.9 °C. The temperature rises above 0 °C only between June and September. The rainfall occurs mainly between June and September, accounting for about 93% of annual precipitation (Zhang et al., 1997). The snowfall is rather scarce in winter owing to dry and cold weather. The annual average

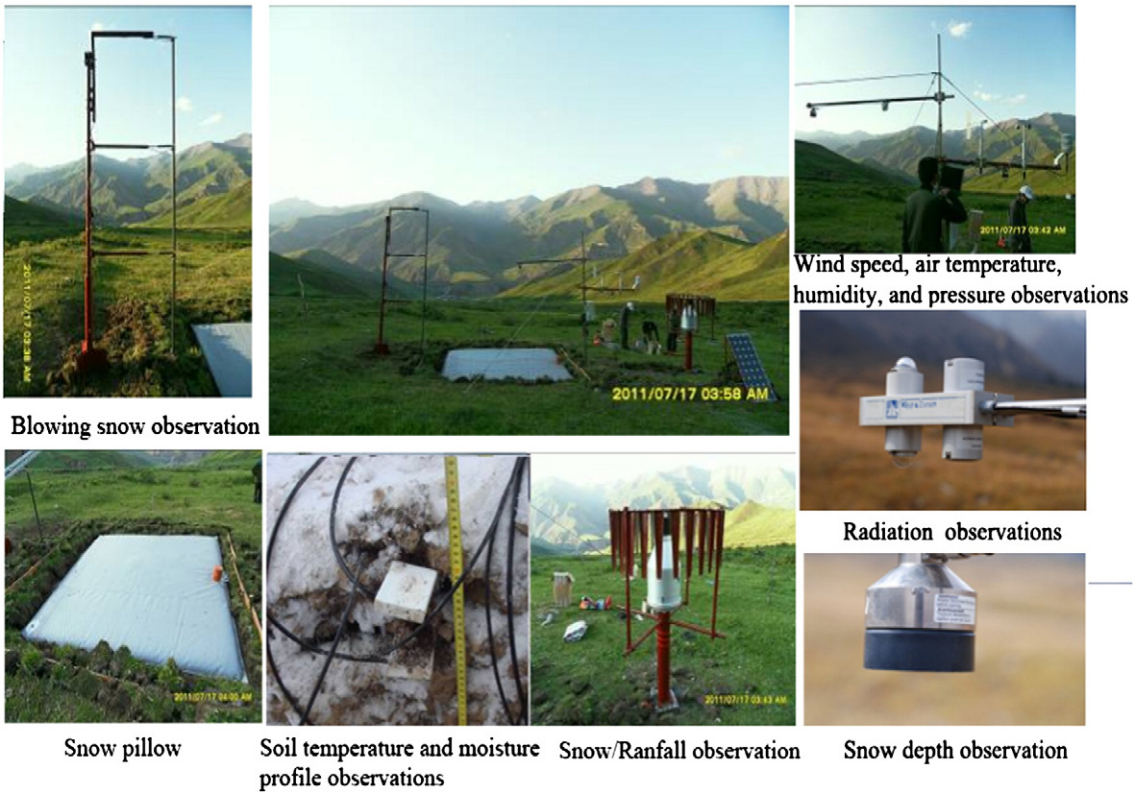

Fig. 2. Binggou research station.

Table 1
Soil properties of Binggou profile derived in laboratory.

Depth	Textural fractions			Bulk density	Organic matter content
	2–0.05 mm	0.05–0.002 mm	<0.002 mm		
(cm)	(%)			(g cm^{-3})	(g kg^{-1})
5	54.79	34.42	10.79	2.44	7.35
10	40.14	47.08	12.78	2.59	6.21
20	35.55	42.70	21.75	2.47	6.76
40	23.45	63.33	13.22	2.63	5.32
80	28.50	58.59	12.91	2.61	5.31
120	87.45	8.29	4.26	2.67	2.33

relative humidity is 65%. The vegetation is rather scarce with grasses of a few centimeters height only. The predominant type of vegetation in the region is *Kobresia humilis* Serg (Ohata et al., 1994). Most of the soil in the non-glacier zone is under permafrost conditions. The surface is frozen in winter and thaws during summer. The depth of the active layer is 1–3 m.

An automatic climate observation system (ACOS) (Fig. 3) was established to measure precipitation, air temperature, wind speed, humidity and radiation (including upward and downward short-wave and long-wave radiations). Eight temperature sensors were installed at depths of 0.1, 0.2, 0.3, 0.4, 0.5, 0.7, 0.9 and 1.1 m. Two heat flux meters were inserted at 0.05 and 0.1 m, and three heat pulse probes at 0.05, 0.1, and 0.15 m. Along with a data logger, these sensors made up the soil monitoring system (SMS). Soil samples were collected from the ground to a depth of 0.9 m at 10 cm intervals below the meteorological station. Table 3 provides details of the main instruments used at this site. The samples were analyzed in the laboratory to determine soil bulk density, and composition with respect to sand, silt, clay, and organic matter content (Table 4).

2.2. Model description

The CoupModel is developed from the previous SOILN model (Eckersten et al., 1998). The CoupModel (Jansson and Karlberg, 2004) is a numerical model for hydrological and thermal processes

Table 2
Main instruments used at Binggou station.

Item	Unit	Instrument	Precision
Air temperature	°C	Humidity and temperature probe (HMD45D, Vaisala Oyj, Finland)	±0.2 °C
Relative humidity	%	Humidity and temperature probe (HMD45D, Vaisala Oyj, Finland)	±2%
Air pressure	hPa	Analog barometer (CS100, Campell, USA)	±0.5 mbar
Wind speed	m s^{-1}	Anemometer (010C-1,MetOne,USA)	±0.11 m/s
Precipitation	mm	Weighing gauge (T-200B, Geonor, Norway)	±0.1 mm
Shortwave radiation	W m^{-2}	Radiometer (CM3, Campell, USA)	±10%
Longwave radiation	W m^{-2}	Infrared radiometer (CG3, Campell, USA)	±10%
Soil temperature	°C	Pt-thermometer (109, Campell, USA)	±0.2 °C
Heat flux in the soil	W m^{-2}	Heat flux plate (PHF01, REBS, USA)	±2%
Snow depth	mm	Ultrasonic level-meter (SR50, CSI, USA)	±10 mm
Blowing snow		Sensor for counting (Flowcapt, ISAW, Switzerland)	±2%

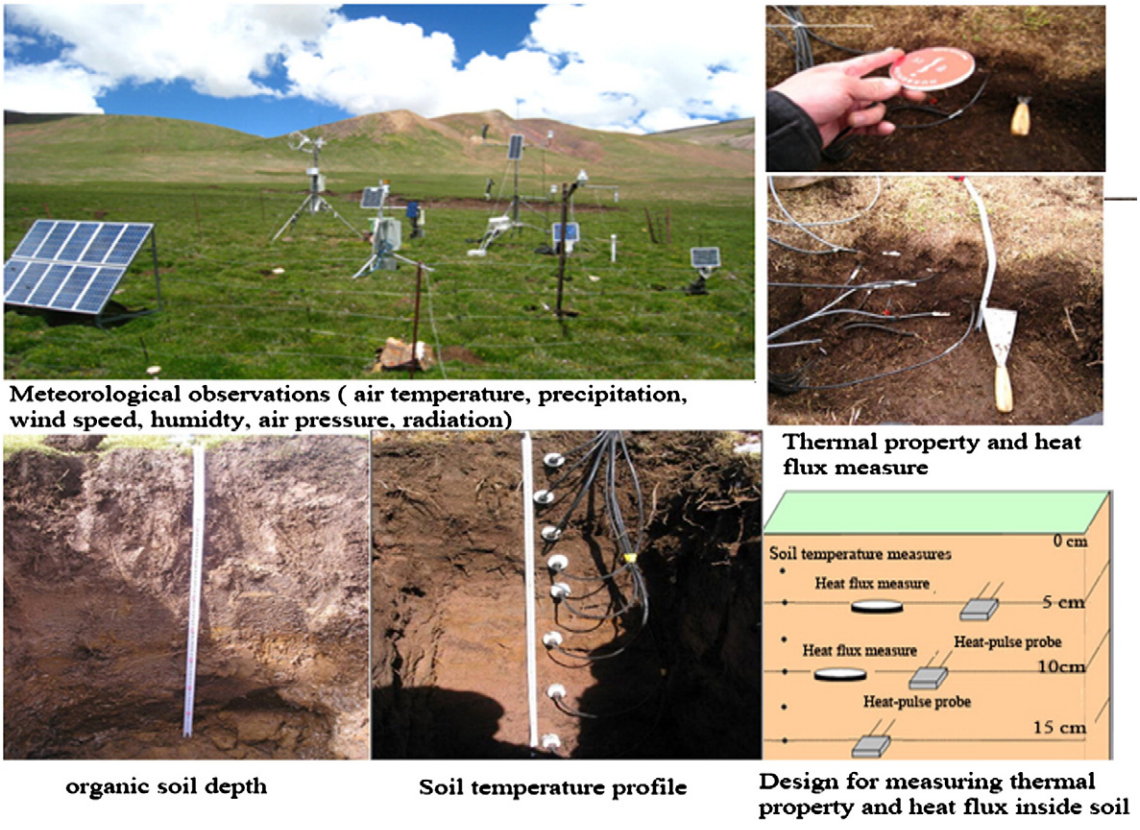

Fig. 3. Tanggula research station.

Table 3
Main instruments used at Tanggula station.

Item	Unit	Instrument	Precision
Air temperature	°C	Humidity and temperature probe (HMD45D, Vaisala Oyj, Finland)	±0.2 °C
Relative humidity	%	Humidity and temperature probe (HMD45D, Vaisala Oyj, Finland)	±2%
Air pressure	hPa	Analog barometer (CS100, Campell, USA)	±0.5 mbar
Wind speed	m s^{-1}	Anemometer (05106, R. M. Young, USA)	±0.3 m/s
Precipitation	mm	Weighing gauge (T-200B, Geonor, Norway)	±0.1 mm
Shortwave radiation	W m^{-2}	Radiometer (CM3, Campell, USA)	±10%
Longwave radiation	W m^{-2}	Infrared radiometer (CG3, Campell, USA)	±10%
Soil temperature	°C	Pt-thermometer (107, Campell, USA)	±0.2 °C
Soil moisture	m^3 m^{-3}	Time-domain reflectometry (CS616, Campell, USA)	±2%
Heat flux in the soil	W m^{-2}	Heat flux plate (HFP01, REBS, USA)	±2%
Thermal conductivity of soil	W m^{-1} C^{-1}	Heat pulse probe (TP02, Hukseflux, Netherlands)	±3% W m^{-1} C^{-1}

in the one-dimensional soil–plant–atmosphere system, especially suited for regions with seasonal snow and frozen soil (Jansson and Halldin, 1979). The CoupModel is an integrated system, consisting of different sub-modules (such as infiltration, evapotranspiration, surface energy balance, heat storage, soil frost, snow dynamics, crop growth, and the C/N cycle). This modular design is advantageous for flexible and objective modeling. The choice of sub-modules generally depends on data availability in the field experiment and on the research objectives.

Meteorological data as the driving variables (including air temperature, surface temperature, precipitation, wind speed, relative humidity and radiation) are input into the model to calculate the heat and water transfer between the subsurface and the atmosphere. The surface temperature and soil evapotranspiration are based on an iterative solution of the surface energy balance including both water and heat fluxes at the soil surface (Alvenäs and Jansson, 1997; Gustafsson et al., 2001). The CoupModel solves the Fourier law of heat conduction including convective flow based on Richard's equation for water flow in the soil layer.

Heat flow q_h to and from each layer is considered to be the sum of conductive and nonconductive heat flow:

$$q_h = -K_h \frac{\partial T}{\partial z} + C_w q_w + L_v q_{vo}$$

where the indices h, v and w mean heat, vapor and liquid water, q is the flux, k the is conductivity, T is the soil temperature, C is the heat capacity, L is the latent heat and z is the depth.

The thermal conductivities are calculated as functions of bulk density, organic content and water/ice content for unfrozen soil and frozen soil, individually. The soil heat capacity equals the weighted sum of the heat capacities of soil constituents (mineral and organic matter, liquid water and ice).

Table 4
Soil properties of Tanggula profile derived in laboratory.

Depth	Textural fractions			Bulk density	Organic matter content
	2–0.05 mm	0.05–0.002 mm	<0.002 mm		
(cm)	(%)			(g cm^{-3})	(g kg^{-1})
10	71	18	11	0.61	166.29
20	66	25	9	0.73	113.7
30	67	21	11	1.13	122.11
40	67	23	10	1.02	128.52
50	52	36	12	1.32	32.58
70	54	32	13	1.39	23.59
90	45	44	11	1.41	25.23

Water flow in the soil is assumed to be laminar and thus obey Richard's equation.

$$q_w = -K_w\left(\frac{\partial \psi}{\partial z} - 1\right) - D_v \frac{\partial c_v}{\partial z} + q_{\text{bypass}}$$

where kw is the unsaturated hydraulic conductivity, ψ is the water tension, z is depth, cv is the concentration of vapor in soil air, Dv is the diffusion coefficient for vapor in the soil and q_{bypass} is a bypass flow in the macro-pores.

The unfrozen soil water retention curve and hydraulic conductivity are calculated alternatively according to Brooks and Corey (1964), and van Genuchten (1980). The mass ratio of frozen water to total amount of water is determined by the soil temperature (below 0 °C) and the freezing point depression curve (sensible and latent heat content of a partially frozen soil). The calculation of the ratio between sensible and latent heat in frozen soil is complicated by a depression of the freezing-point. The soil water potential and hydraulic conductivity are revised by the water/ice content for frozen soil. A detailed technical description of the model is given by Jansson and Karlberg (2004).

Snow processes are considered in their role as water storage, boundary condition for soil water flows, and important factor influencing the soil heat boundary condition. The CoupModel is capable of incorporating interface processes connected with snow. The entire snow pack is considered to be homogeneous both horizontally and vertically.

The heat flux between snowpack and soil is calculated:

$$q_1 = {}^{2k_{\text{snow}}k_{h1}(T_{\text{snow}}-T_1)}\Big/_{(k_{\text{snow}}\Delta Z_1 + k_{h1}\Delta Z_{\text{snow}})}$$

where k_{h1}, ΔZ_1 and T_1 is the thermal conductivity, thickness and temperature of the upper most soil layer, respectively.

Snow surface heat flux is calculated:

$$q_2 = {}^{2k_{\text{snow}}(T_{\text{snows}}-T_{\text{snow}})}\Big/_{Z_{\text{snow}}}$$

where T_{snows} is the snow surface temperature, T_{snow} is the temperature of the snow pack, k_{snow} is the thermal conductivity of the snow and z_{snow} is the snow depth.

Snow thermal conductivity, k_{snow} is sensitively related to snow density, ρ_{snow} (Snow Hydrology, 1956):

$$k_{\text{snow}} = s_k \rho_{\text{snow}}^2$$

where s_k, SthermalCondCoef, is an empirical parameter.

Snow melt is calculated using an empirical melting/freezing function based on global radiation, air temperature and the heat flux to and from the soil (Jansson and Karlberg, 2004).

Another advantage of the CoupModel is its use of the Bayesian (Klemedtsson et al., 2008) and the GLUE calibrating approaches

(Lundmark, 2008), which allow to quantify the parameter uncertainties in the model. The assumed prior parameter ranges can be reduced through the Markov Chain Monte Carlo (MCMC) method, thus reducing the uncertainty in the simulation. Information about development and use of the CoupModel is available from the internet (http://www.lwr.kth.se/vara%20datorprogram/ CoupModel/index.htm).

The CoupModel has been widely applied to simulate soil heat and water processes under different snow and soil freezing and thawing conditions in many areas of the world. Keller et al. (2004) used the CoupModel to evaluate the influence of the snow pack on soil thermal conditions in a sub-alpine ski resort in central Switzerland. Mellander et al. (2005) studied snow pack and soil temperature variation in the boreal forest landscape of northern Sweden with the CoupModel and concluded that the extent and duration of snow pack strongly influences the timing and rapidity of soil warming in spring. Yang et al. (2010) simulated the influence of alpine meadow vegetation on the heat and water transfer processes of seasonally frozen soil in the mountains of Northwest China. Moreover, the model was used to predict the active layer thickness under future warming scenarios in Greenland (Hollesen et al., 2011). Therefore, we selected the CoupModel in our study for simulating the influence of snowpack and organic soil on active layers at the two monitoring field sites.

2.3. Model application

2.3.1. Binggou station

The CoupModel was first calibrated to reproduce the current daily variation of soil temperature at different depths as well as the depth of snow cover at Binggou station. The simulation time period was from October 30, 2007 to July 20, 2009. The computation time step was a day. The local meteorological station provided input variables (wind speed, air temperature, humidity, precipitation, and incoming solar radiation) for the simulation. The soil profile was set to be 10.0 m deep and was subdivided into 27 layers with layer thicknesses increasing from 0.02 m at the top to 1.0 m at 10 m depth. At the bottom of the profile, a constant temperature boundary was set to −1.2 °C obtained from observation in the temperature measuring hole. In the upper 1.3 m, the thickness of each layer was selected such that centers of layers coincided with the measuring depths of soil temperatures.

The density of new snow and thermal conductivity of snowpack were calibrated with the GLUE approach by validation of measured soil temperatures and snow depth. A total of 8000 simulations were run and sampling was carried out according to the MCMC chain using a step length of 0.05. The density of new snow, DensityCoefWater, ranged between 100 and 200 kg/m^3. The thermal conductivity of snowpack is proportional to the square of the snowpack density (Snow Hydrology, 1956). The proportionality coefficient, SthermalCondCoef, ranged from 10^{-6} to $2.8 \cdot 10^{-6}$.

The model was used to simulate the sensitivity of the active layer thickness to a warming climate. Four scenarios for future climate change were conducted, increasing the annual mean air temperature by 1 °C, 2 °C, 4 °C, and 6 °C, respectively. To investigate the effect of increasing amounts of precipitation and snow depth on active layer thickness, the model was also run with 30% and 100% more precipitation and ignoring snow pack in winter.

2.3.2. Tanggula station

The CoupModel was used to simulate the influence of organic soil on the active layer based on monitoring at Tanggula station. The simulation time period was from July 1, 2006 to May 9, 2011. Daily mean values of air temperature, precipitation, wind speed, relative humidity and global radiation were used as input into the model. The soil profile was also set to be 10.0 m deep and was subdivided into 27 layers with layer thicknesses increasing from 0.05 m at the top to 1.0 m at 10 m depth. In the upper 1.2 m, the thickness of each layer was selected such that the center of each layer coincided with the measuring depths of soil temperature. A constant temperature boundary at the bottom was set to −1 °C corresponding to warm permafrost on QTP, with annual mean ground temperatures usually between −0.5 °C and −1 °C.

Three types of parameters, which are the heat capacity and the thermal conductivity for each dry soil layer, and the organic layer thickness, were calibrated with the Bayesian approach on the basis of measured soil temperatures. A total of 5000 simulations were run and sampling was carried out according to the MCMC method using a step length of 0.05. The prior ranges of the parameters used in the calibration were set sufficiently wide to embrace the full range of all likely values. To adjust the thermal conductivity individually for each dry soil layer, a scaling coefficient is applied, which relates the layer value to the default value (Jansson and Karlberg, 2004). The scaling coefficients ranged from 0 to 1.6. Similarly the layer heat capacity was adjusted starting out from a prior distribution ranging from 1.8 MJ/m^3 to 4 MJ/m^3. The prior organic layer thickness ranged from 0 m to1 m.

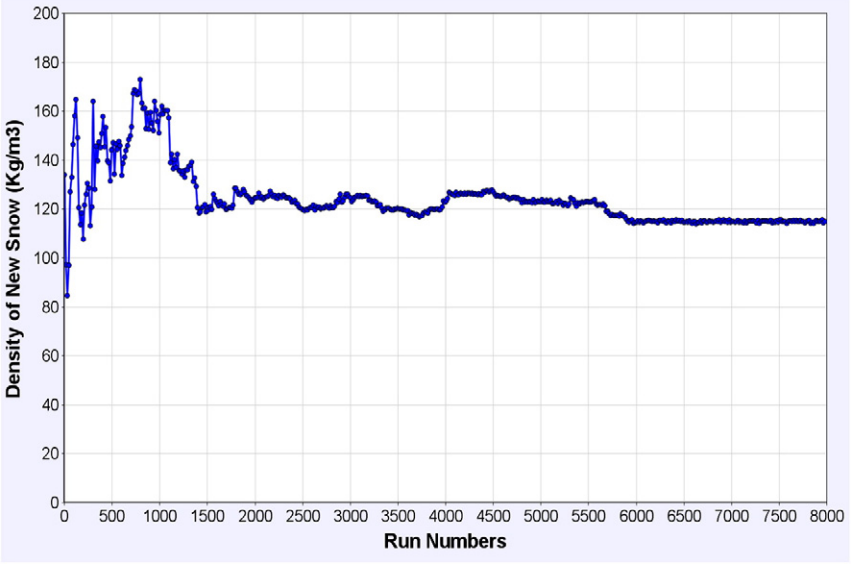

Fig. 4. Calibration of snow density with the Bayesian method (Binggou) (8000 simulations).

Table 5
Statistics of observed and simulated snow depths, soil heat fluxes and soil temperatures (Binggou).

	Snow depth	Heat flux	Soil temperatures				
Depth		5 cm	10 cm	20 cm	40 cm	80 cm	120 cm
NSE	0.76	0.65	0.950	0.95c4	0.937	0.913	0.910
RMSE	0.038 m	0.37 MJ/day	0.86 °C	0.74 °C	1.07 °C	0.90 °C	0.98 °C
ME	0.026 m	−0.11 MJ/day	−0.02 °C	−0.02 °C	−0.20 °C	−0.16 °C	0.17 °C
R^2	0.87	0.72	0.951	0.955	0.942	0.916	0.932

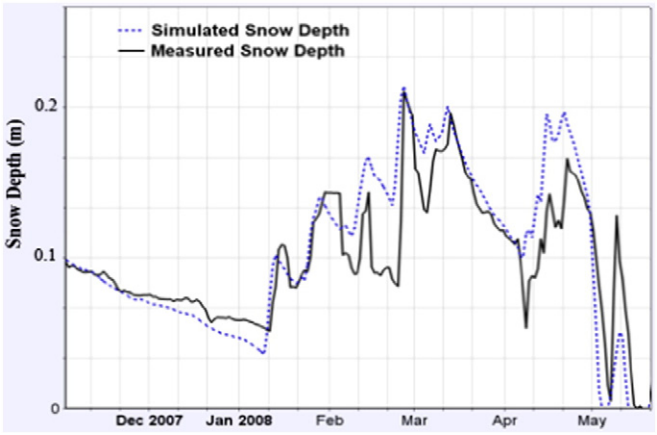

Fig. 5. Simulated and observed snow depths (Binggou).

Based on the validated model, an investigation into the influence of the organic layer on the active layer was conducted by comparing modeled soil temperature profiles under different organic layer depth scenarios, corresponding to depths of 20 cm, 40 cm, and 80 cm, and ignoring the organic layer. Simulations were performed for the scenario 'ignoring the organic layer' by replacing the calibrated parameters of the upper 0.4 m of soil profile with the default mineral-soil heat capacity of 2 MJ/m^3 and the default scaling coefficient of the mineral-soil thermal conductivity of 1.0.

In this study, model performance was evaluated on the basis of the coefficient of determination for a linear regression between simulated and observed values (R^2), the mean error (ME), the root mean square error (RMSE), and the Nash–Sutcliffe coefficient (NSE). The latter are calculated as:

$$\mathrm{ME} = \frac{1}{N}\sum_{i=1}^{N}\left(X_{sim,t} - X_{obs,t}\right)$$

$$\mathrm{RMSE} = \frac{1}{N}\sqrt{\sum_{t=1}^{N}\left(X_{sim,t} - X_{obs,t}\right)^2}$$

$$\mathrm{NSE} = 1 - \left(\sum_{t=1}^{N}\left(X_{sim,t} - X_{obs,t}\right)^2 / \sum_{t=1}^{N}\left(X_{obs,t} - \overline{X}\right)^2\right)$$

where N is the number of observations, $X_{obs,t}$ and $X_{sim,t}$ are the observed and simulated values, respectively.

3. Results and discussion

3.1. Binggou station

The calibration process of new snow density with the GLUE approach is presented in Fig. 4. The calibrated new snow density of 119 kg/m^3 is very similar to the observed values from March 25 to May 15, 2008, which range between 108 kg/m^3 and 126 kg/m^3. The calibrated parameter, SthermalCondCoef, is determined as $1.8 \cdot 10^{-6}$ with the same approach.

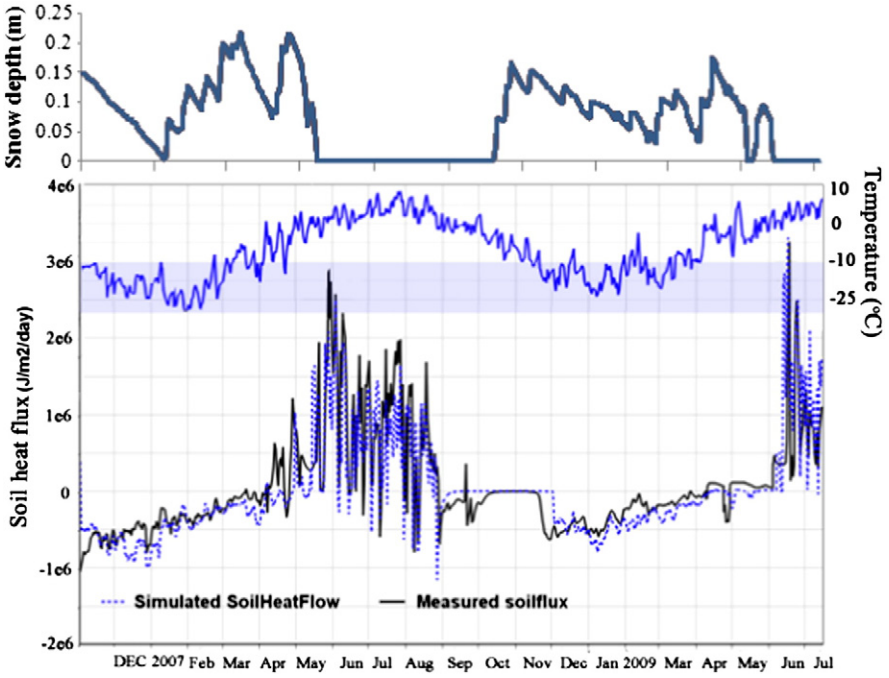

Fig. 6. Simulated and observed ground heat fluxes at 2 cm depth (Binggou).

Table 5 summarizes the model performance. Fig. 5 shows the comparison between simulated and observed snow depths from October 30, 2007, to May 20, 2008. The model performed well in reproducing the measured snow depth. The coefficient of determination for the linear regressions is 0.87. The RMSE and NSE values are 0.038 m and 0.76, respectively. The ME (0.026 m) reveals that snow depth was systematically overestimated. This systematic overestimation is considered to be a result of ignoring snow mass losses due to blowing snow and snowpack sublimation.

The direction and magnitude of the ground heat flux, which are decided by the temperature gradient and thermal properties of the medium at the atmosphere–soil interface, affect soil freeze/thaw cycles. Observations show that when air temperature was more than 0 °C and the snow pack disappeared in the middle of May, 2008, the ground heat flux from atmosphere to soil increased significantly (Fig. 6). When air temperature decreased to 0 °C in August 28, 2008, and precipitation led to snow on the ground, the ground heat flux rapidly decreased approaching zero (Fig. 6) and remained there for a long time until air temperature decreased to less than −10 °C in the middle of November, 2008 (Fig. 6). The snowpack prevented the energy transfer between the atmosphere and the soil, and the soil temperature during the period was controlled by the snow depth, which acted as an insulator and resulted in soil temperature values near 0 °C above the depth of 120 cm (Fig. 7). When air temperature was less than −10 °C from mid-November, 2008, to March, 2009, further cooling of the soil profile occurred, and the soil temperature during the period was controlled by the air temperature near land surface. Subsequently, the air temperature increased to more than −10 °C in April, 2009, and the ground heat flux was near zero again until the snow pack disappeared in the beginning of June, 2009. So, from the observed data, we conclude that the role of snow is crucial to the energy transfer between the atmosphere and the soil at Binggou station. The −10 °C air temperature in winter is a threshold for whether soil temperature is mainly controlled by air temperature or by shallow snow at Binggou station.

The comparison between the simulated ground heat flux and observations is shown in Fig. 6. The results show that the CoupModel performs well in simulating ground heat flux, with a coefficient of determination of 0.72 and an NSE of 0.65, respectively (Table 5). The RMSE and ME values are 0.37 MJ/day and −0.11 MJ/day, respectively

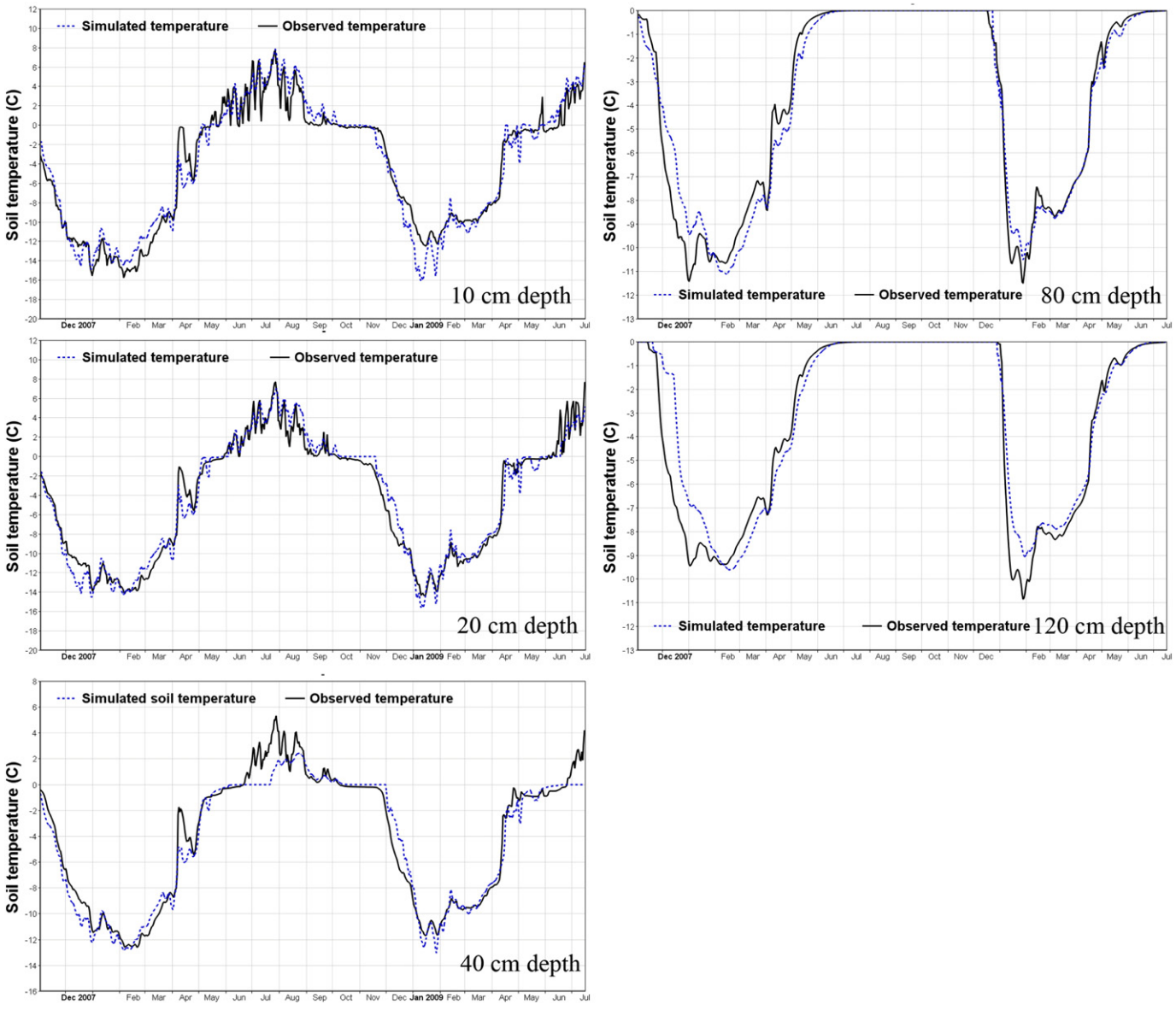

Fig. 7. Simulated and observed soil temperatures (Binggou).

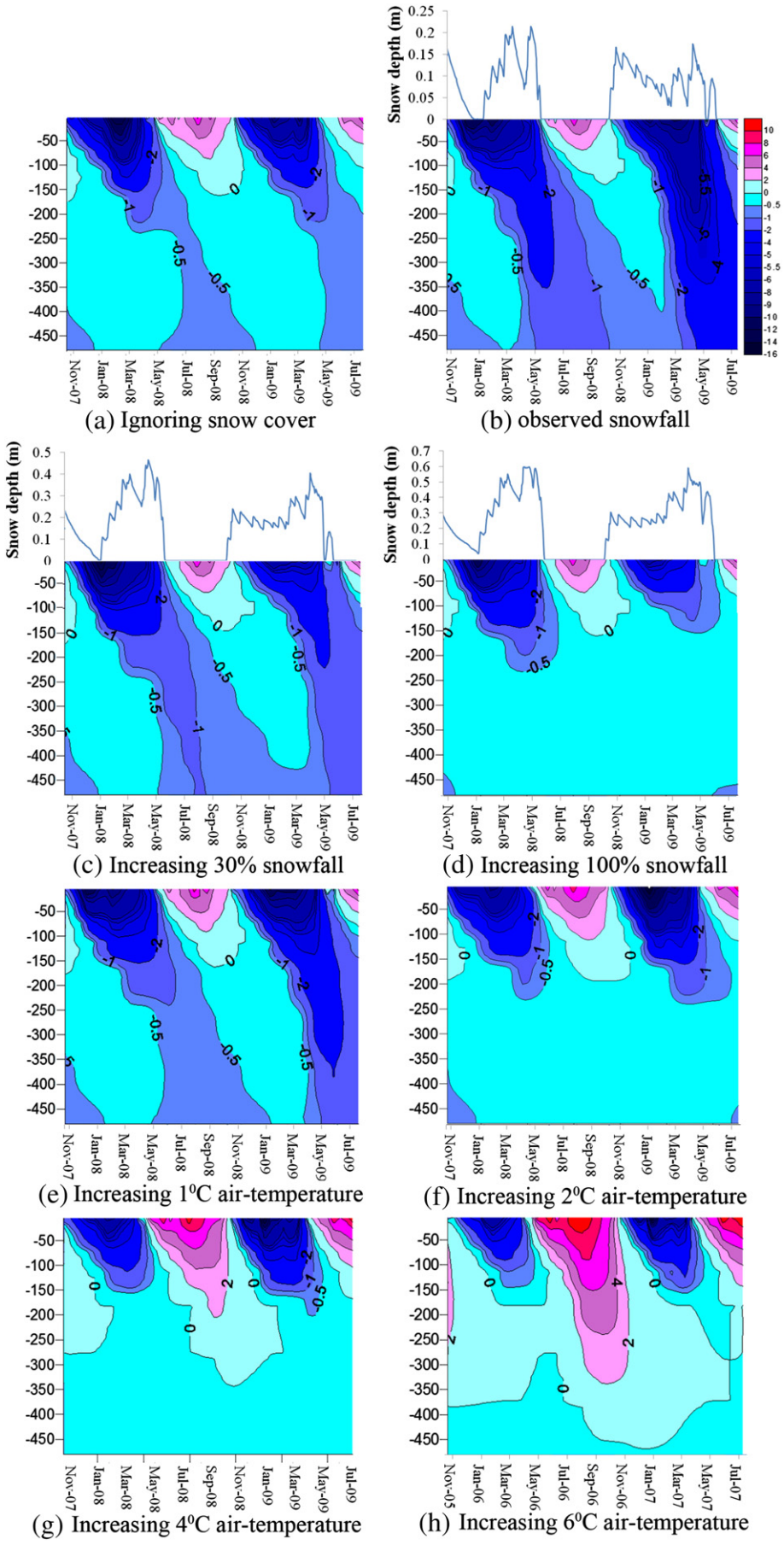

Fig. 8. Simulated isothermals of soil profile for different climate change scenarios (Binggou).

Table 6
Simulated cumulative ground heat flux during a freezing/thawing cycle period for different climate change scenarios (Binggou).

Current air-temperature	Cumulative ground heat flux (MJ/m^2)			
	Ignoring snow cover	Current snowfall and snow depth	Increasing snowfall by 30%	Increasing snowfall by 100%
Thawing period (May 1, 2008–Oct. 1, 2008)	122.9	130.73	120.28	112.88
Freezing period (Oct. 1, 2008–May 1, 2009)	−155.7	−201.94	−168.17	−143.69
Current precipitation	Increasing air-temperature by 1 °C	Increasing air-temperature by 2 °C	Increasing air-temperature by 4 °C	Increasing air-temperature by 6 °C
Thawing period (May 1, 2008–Oct. 1, 2008)	133.12	140.10	152.08	156.44
Freezing period (Oct. 1, 2008–May 1, 2009)	−191.73	−183.51	−164.50	−144.43

(Table 5). The model also performed very well for the entire period from October 30, 2007, to July 20, 2009, in reproducing soil temperature (Fig. 7, Table 5). The coefficients of determination for the linear regression range from 0.916 to 0.955 and NSEs are close to unity (0.91 to 0.954). The mean temperature differences (ME) were less than 0.2 °C. The results indicate that the calibrated scaling coefficients of thermal conductivity for snowpack are reasonable at the study site. In summary, the CoupModel can be used to quantitatively simulate the snowpack change and the effect for seasonal variations of soil temperatures.

Based on the calibrated model, an investigation into the influence of climatic warming on the active layer was conducted by comparing modeled soil temperature profiles under four scenarios for increasing annual mean air temperature. The results are shown in Fig. 8 and reveal that the maximum active layer thickness at Binggou station may increase by about 20, 50 or 200 cm compared to the current 150 cm active layer thickness, depending on whether an air temperature increase by 1 °C, 2 °C, or 4 °C respectively was used. A talik forms at the top of the permafrost as a result of a 6 °C warming, while the simulated cumulative ground heat loss to the atmosphere (156.44 MJ/m^2) is more than the simulated cumulative heat transfer from the atmosphere to the soil (−144.43 MJ/m^2) during a freezing/thawing cycle period (Table 6). The length of the summer thawing period, defined by zero or above zero surface temperatures, is extended by 10 days in 1 °C increasing scenario, 25 days in 2 °C increasing scenario, 46 days in 4 °C increasing scenario, and 58 days in 6 °C increasing scenario compared with current soil temperatures. The sensitivity of the active layer thickness with respect to snow depth was assessed by applying 30% and 100% more precipitation and 0 mm precipitation (no snowfall) compared to current precipitation in winter. The results are shown in Fig. 8 and reveal that the soil freezes deeper with snow depth less than 20 cm in the present climate, than in the case of ignoring snow cover. The increased albedo in winter, due to snow cover, reduces net shortwave radiation absorbed by the soil–snow system (Fig. 9) and energy heating land surface, and results in reduction of snow surface temperature (Fig. 10). Both the lower snow surface temperature and smaller heat conductive effects with a thin snow cover result in the increase of the energy loss from soil to the atmosphere in the winter. The simulated cumulative ground heat flux during the freezing period is −155.7 MJ/m^2 when ignoring snow pack, which is less than what was obtained for a surface covered by shallow snow under present conditions, which is −201.94 MJ/m^2 (Table 6). However, this positive effect is lost with the increased precipitation and snow depth in winter. The decrease of simulated cumulative ground heat flux during the freezing period along with thicker snow depths (Table 6) indicates that the thicker snow pack gradually insulates the subsoil against energy losses to the atmosphere, which induces the reduction of active layer frozen depth. Based on the above analysis, we conclude the shallow snow pack (less than 20 cm) contributes to the conservation of permafrost, while the deep snow pack (more than 20 cm) is not conducive to the maintenance of permafrost at Binggou station.

3.2. Tanggula station

The calibration process of organic layer thickness with the Bayesian method is presented in Fig. 11. The calibrated organic layer thickness is 0.4 m, which is very similar to our observation (0.4 m–0.5 m organic layer thickness). The calibrated values of scaling coefficients of the dry soil thermal conductivity ranged from 0.3 to 0.7 in the upper 0.4 m, and from 0.6 to 1.6 at 0.4–8 m depth. The calibrated values of dry soil

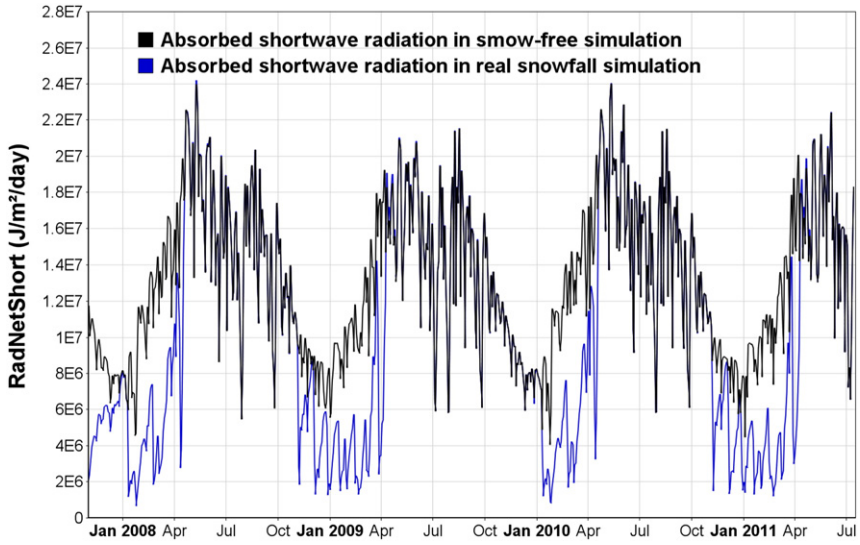

Fig. 9. Comparison of simulated shortwave radiation absorbed by the soil–snow system between in snow-free and in current snowfall.

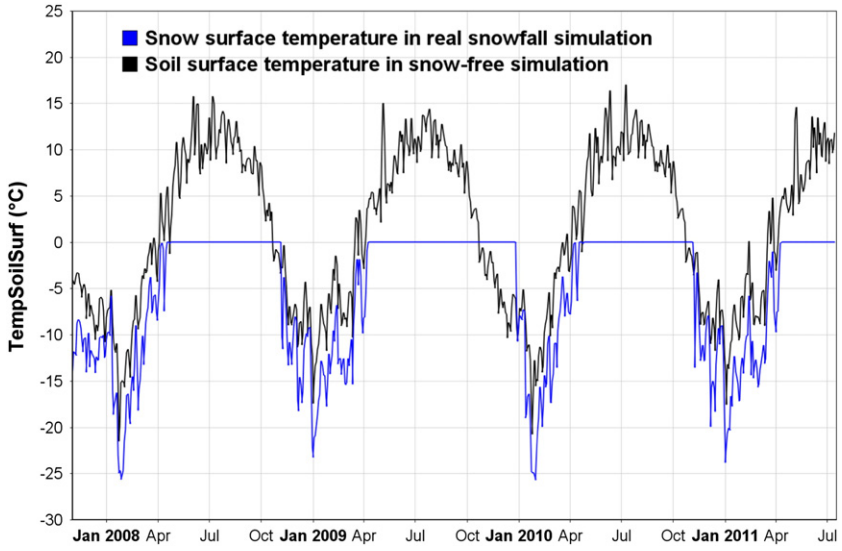

Fig. 10. Comparison of simulated bare-soil surface temperature in snow-free and snow surface temperature in current snowfall.

heat capacity range from 2.3 to 4.0 MJ/m^3 in the upper 0.4 m, and from 1.83 to 2.39 MJ/m^3 at 0.4–8 m depth. The reason for the lower thermal conductivity and the higher heat capacity in the upper soil layers is most likely the higher content of organic matter.

Simulated soil temperatures are shown within the 90% accepted runs describing the model uncertainty. Fig. 12 shows that mean simulated soil temperatures agreed well with the measurements. Table 7 summarizes the model performance. The coefficients of determination for the linear regressions range from 0.926 to 0.951 and NSE coefficients are close to unity, ranging from 0.913 to 0.942. The maximum mean temperature differences (ME) are less than 0.8 °C. The calibrated parameters for each soil layer are reasonable for the local soil properties at the study site. The comparison of soil temperatures at different depths (Fig. 12) shows that the duration of soil temperatures close to 0 °C is prolonged along with increasing soil depth in winter. The difference between the speed of soil temperature decreases in the freezing period and that of soil temperature increases in the thawing period is gradually larger with increasing soil depth. The reason is that the thermal conductivity of ice is larger than the thermal conductivity of water. During the soil freezing period, the thermal conduction increases with increasing ice content of the upper soil layer. On the contrary, during the soil thawing period, the thermal conduction decreases with increasing water content of the upper soil layer. We conclude that the CoupModel can successfully simulate seasonal variations of soil temperatures along with phase changes, also for the case where a layer of high content of organic matter is lying above a mineral soil.

The comparison of simulated soil isothermals from May 1, 2009, to May 9, 2011, for different organic layer depths is shown in Fig. 13. The model results reveal that the maximum thawing depth for the active layer in summer is close to 300 cm when ignoring the organic layer. However, it is less than 150 cm with a realistic organic layer of 40 cm depth. The simulated thawing depth gradually decreases with the increase of the soil organic layer depth. The simulated isothermals in winter move upward along with the increase of the soil organic layer depth. The causes of these phenomena are the low thermal conductivity

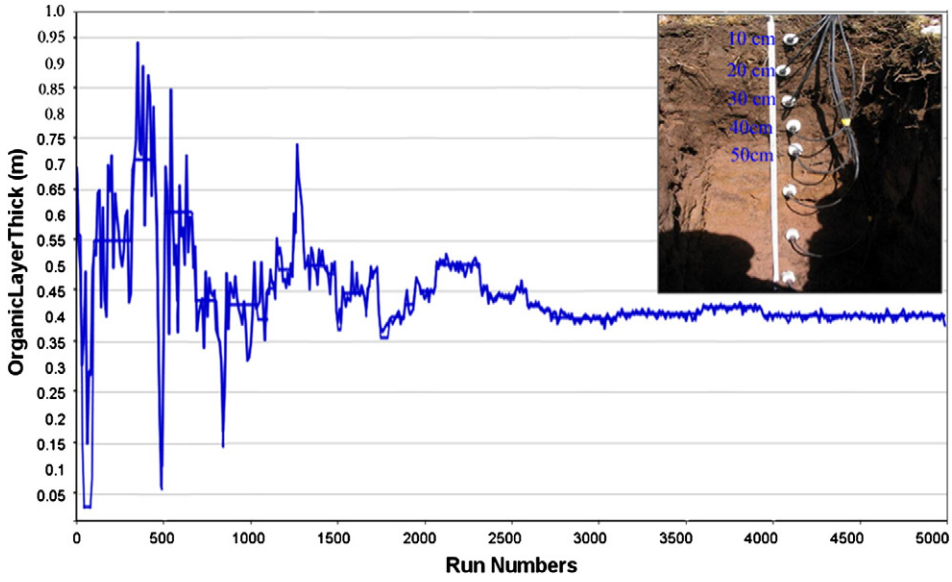

Fig. 11. Calibration of organic layer thickness with the Bayesian method (Tanggula) (5000 simulations).

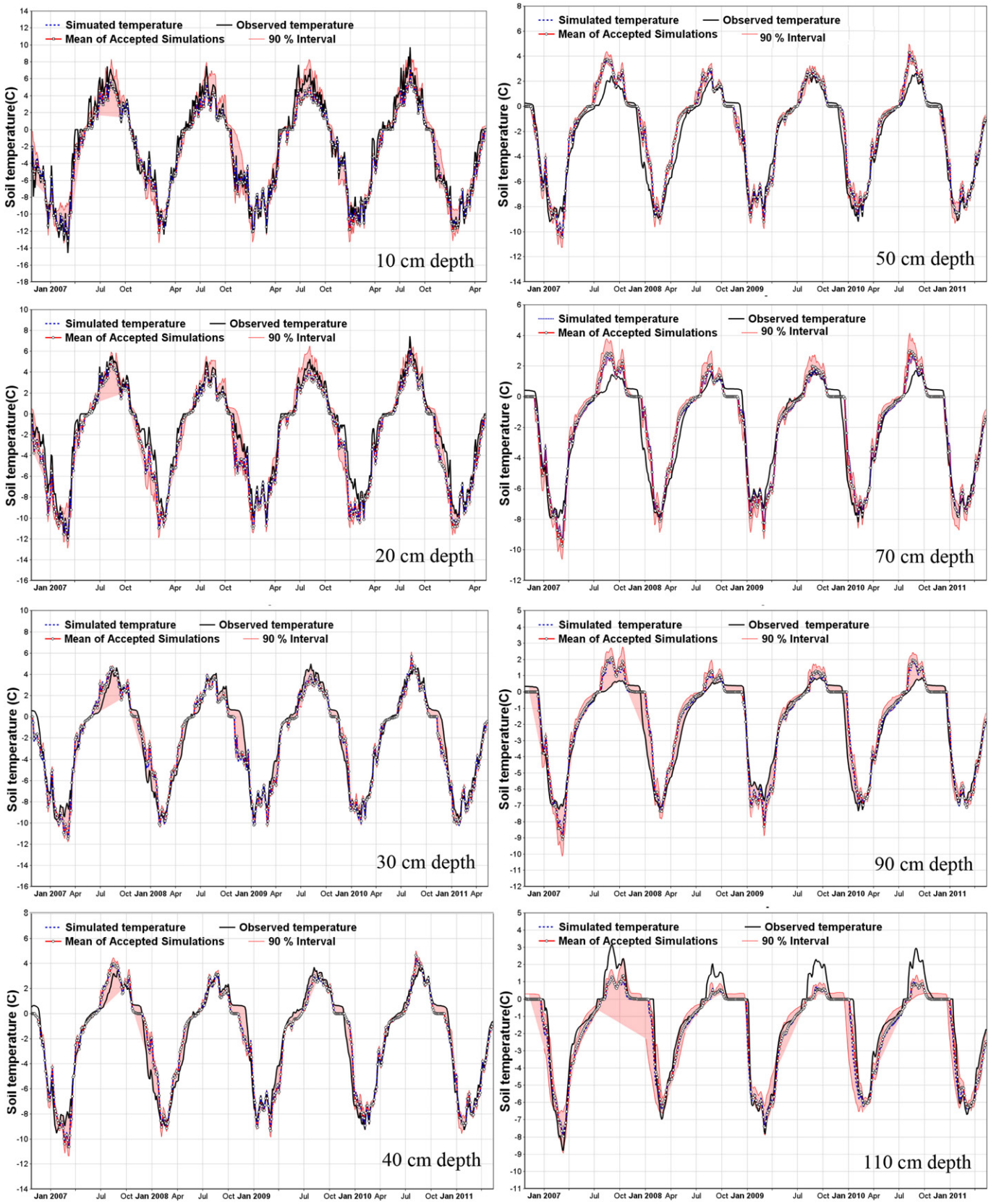

Fig. 12. Simulated and observed soil temperatures (Tanggula).

and the high heat capacity of the organic layer, which make the underlying soil less responsive to solar radiation and air temperature fluctuations. We conclude that the soil organic layer in winter reduces the heat loss from the deeper soil layers to the atmosphere. Meanwhile, in summer it reduces similarly the heat transfer from the atmosphere to the deeper soil layers and leads to a shallower active layer melting depth.

Table 7
Statistics of observed versus simulated mean soil temperatures (Tanggula).

	Soil temperatures							
Depth	10 cm	20 cm	30 cm	40 cm	50 cm	70 cm	90 cm	110 cm
NSE	0.927	0.937	0.938	0.942	0.937	0.935	0.921	0.913
RMSE	1.4 °C	1.2 °C	1.1 °C	0.86 °C	0.89 °C	0.76 °C	0.73 °C	0.75 °C
ME	−0.8 °C	−0.6 °C	−0.3 °C	−0.07 °C	−0.3 °C	−0.06 °C	−0.05 °C	0.01 °C
R^2	0.938	0.947	0.944	0.951	0.949	0.941	0.934	0.926

In summary, the soil organic layer reduces the response of the active layer to external factors, and contributes to the conservation of permafrost.

4. Conclusions

The QTP is characterized by a normally shallow snow depth in winter and an extensive distribution of tundra soils. The main objective of this study was to investigate into the influence of snow pack and organic soil thickness on the active layer on the QTP through monitoring and numerical modeling. Two typical field sites (Binggou station and Tanggula station) on the QTP were established to monitor the impact of snow and organic soil, respectively, on the energy balance and thermal states within active layer. The calibrated model results demonstrated that the CoupModel can successfully describe the seasonal dynamics of the active layer under consideration of snow pack and organic soil conditions.

Based on the calibrated model, a sensitivity analysis with respect to the influence of climatic warming on the active layer at Binggou station was performed. Using the model for predicting changes in the active layer in response to a 1–6 °C warming indicates that the maximum active layer thickness may increase from today 150 cm to about 350 cm as a result of a 4 °C warming. The permafrost starts to develop and permafrost will thaw as a result of a 6 °C warming at Binggou station (altitude 4146.4 m a.s.l.). Using the model for predicting changes in the active layer as a response to snow depth under different precipitation scenarios in winter, the results indicate that 20 cm snow depth is the threshold for contribution to the conservation of permafrost in winter. More than 20 cm snow depth in winter is not conducive to the maintenance of permafrost at Binggou station.

Based on the calibrated model, a sensitivity analysis with respect to the influence of the organic soil layer depth to the active layer at Tanggula station was performed. Using the model for predicting changes in the active layer as a response to different soil layer depths indicates that the maximum thawing depth in summer may increase from 150 cm with realistic 40 cm organic layer to almost 300 cm as a result of ignoring the organic soil layer. The simulated isothermals in winter move upward along with the increase of the soil organic layer depth. An organic layer makes the underlying soil less responsive to fluctuations in solar radiation and air temperature due to is low thermal conductivity and high heat capacity. It reduces the rate of the active layer deepening under future climatic warming.

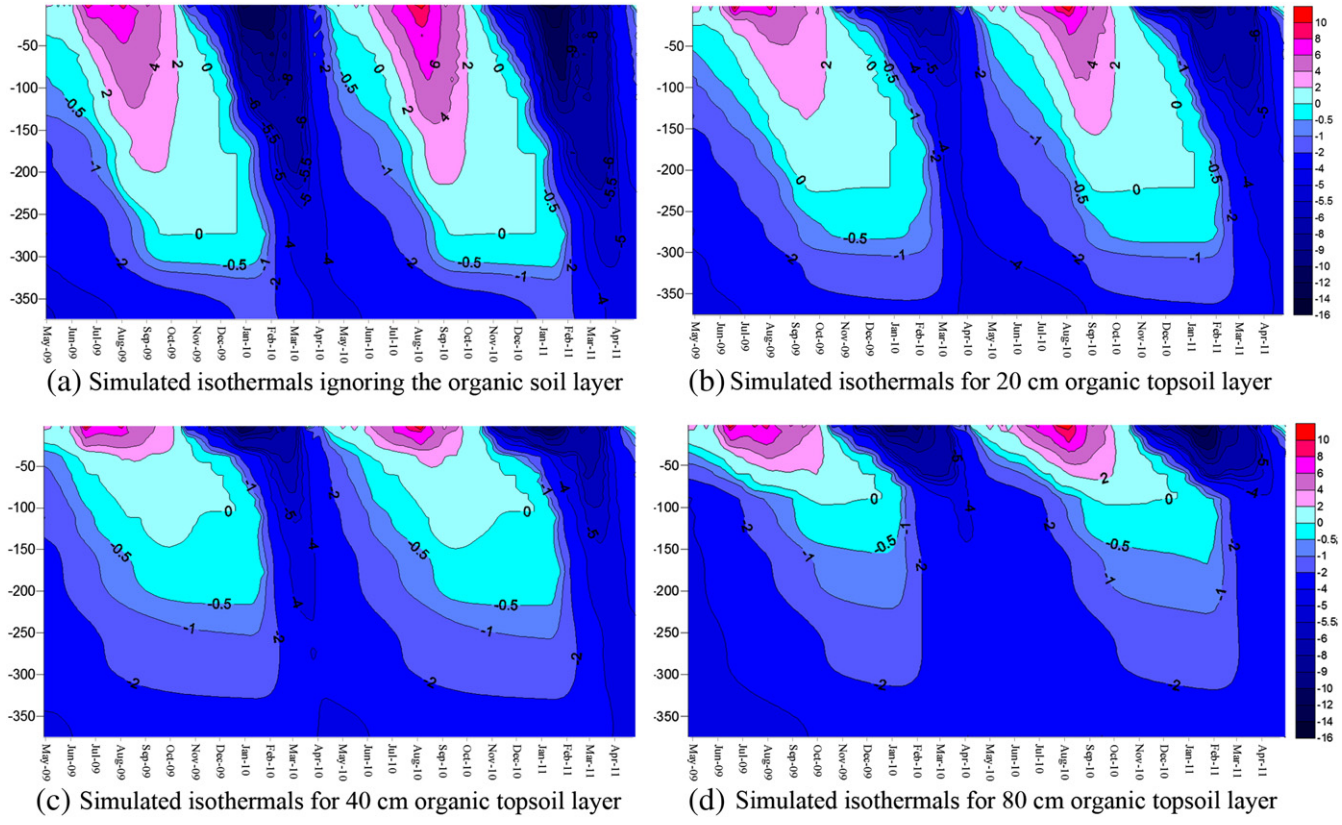

Fig. 13. Simulated isothermals of soil profile for different organic layer depth scenarios (Tanggula).

In summary, snow pack and organic layer have a considerable influence on the seasonally frozen soils of the QTP. Warmer climatic conditions may result in good vegetation cover and an increased organic content of soil, leading to a shallower active layer. On the other hand, the observed increase in snow on the QTP over the last 50 years (Li et al., 2008; Yang et al., 2008), has certainly decreased the active layer frozen depth in winter and accelerated permafrost degradation. These different conclusions indicate that soil temperature responses to future climatic change will likely be complicated by the impact of climatic change on snow, surface vegetation cover and soil organic layer properties.

Acknowledgments

This work is supported by the NSFC (National Science Foundation of China) projects (grant number: 91125023). SSSTC (Sino Swiss Science and Technology Cooperation Program) project (grant number: IP14-092010) and State Key Laboratory of Frozen Soil Engineering, Cold and Arid Regions Environmental and Engineering Research Institute, Chinese Academy of Sciences (grant number: SKLFSE201005). Gratitude is expressed to Binggou and Tanggula experimental stations for collecting data under difficult conditions.

References

Allison, I., Barry, R.G., Goodison, B.E., 2001. Climate and Cryosphere (CliC) Project. Science and Co-ordination Plan, Version 1. I., World Climate Research Programmer, WCRP-114, WMO/TD No. 1053, Geneva, p. 76.

Alvenäs, G., Jansson, P.-E., 1997. Model for evaporation, moisture and temperature of bare soil: calibration and sensitivity analysis. Agricultural and Forest Meteorology 88, 47–56.

Anisimov, O.A., Shiklomanov, N.I., Nelson, F.E., 1997. Global warming and active-layer thickness: results from transient general circulation models. Global and Planetary Change 15, 61–78.

Brooks, R.H., Corey, A.T., 1964. Hydraulic Properties of Porous Medium. Hydrology Paper No. 3. Colorado State University, Fort Collins, Colorado (27 pp.).

Brown, J., Nelson, F.E., Hinkel, K.M., 2000. The Circumpolar Active Layer Monitoring (CALM) program research designs and initial results. Polar Geography 3, 165–258.

Cheng, G.D., 1984. Problems on zonation of high-altitude permafrost. Acta Geographical Sinica 39, 185–193 (In Chinese with English abstract).

Cheng, G.D., 2005. A roadbed cooling approach for the construction of Qinghai–Tibet Railway. Cold Regions Science and Technology 42, 169–176.

Cheng, G.D., Wu, T.H., 2007. Responses of permafrost to climate change and their environmental significance, Qinghai-Tibet Plateau. Journal of Geophysical Research 112, F02S03. http://dx.doi.org/10.1029/2006JF000631.

Coordinated Energy and Water-cycle Observations Project (CEOP), 2008. Strategic Implementation Plan. http://www.ceop.net/.

Eckersten, H., Jansson, P.-E., Johnson, H., 1998. SOILN Model, ver. 9.2, User's Manual. Division of Hydrotechnics, Communications 98:6. Department of Soil Sciences, Swedish Agricultural University, Uppsala (113 pp.).

Frauenfeld, O.W., Zhang, T.J., Barry, R.G., Gilichinsky, D., 2004. Interdecadal changes in seasonal freeze and thaw depths in Russia. Journal of Geophysical Research 109. http://dx.doi.org/10.1029/2003JD004245 D05101.

Goodison, B.E., Brown, R.D., Grane, R.G., 1998. EOS Science Plan: Chapter 6, Cryospheric System. NASA.

Gustafsson, D., Stähli, M., Jansson, P.-E., 2001. The surface energy balance of a snow cover: comparing measurements to two different simulation models. Theoretical and Applied Climatology 70, 81–96.

Hinzman, L.D., Kane, D.L., Yoshikawa, K., Carr, A., Bolton, W.R., Fraverv, M., 2003. Hydrological variations among watersheds with varying degrees of permafrost. Proceedings of the Eighth International Conference on Permafrost, 21–25 July 2003. Balkema Publishers, Zurich, Switzerland, pp. 407–411.

Hollesen, J., Elberling, B., Jansson, P.E., 2011. Future active layer dynamics and carbon dioxide production from thawing permafrost layers in Northeast Greenland. Global Change Biology 17, 911–926.

Jansson, P.-E., Halldin, S., 1979. Model for the annual water and energy flow in a layered soil. In: Halldin, S. (Ed.), Comparison of Forest and Energy Exchange Models. Society for Ecological Modelling, Copenhagen, pp. 145–163.

Jansson, P.-E., Karlberg, L., 2004. Coupled Heat and Mass Transfer Model for Soil–Plant–Atmosphere Systems. Royal Institute of Technology, Department of Civil and Environmental Engineering, Stockholm, Sweden, pp. 1–435.

Kane, D.L., Hinzman, L.D., Zarling, J.P., 1991. Thermal response of the active layer to climate warming in a permafrost environment. Cold Regions Science and Technology 19, 111–122.

Keller, T., Pielmeier, C., Rixen, C., Gadient, F., Gustafsson, D., Stähli, M., 2004. Impact of artificial snow and ski-slope grooming on snowpack properties and soil thermal regime in a sub-alpine ski area. Annals of Glaciology 38, 314–318.

Kimball, J.S., McDonald, K.C., Keyser, A.R., Frolking, S., Running, S.W., 2001. Application of NASA scatterometer (NSCAT) for determining the daily frozen and nonfrozen landscape of Alaska. Remote Sensing of Environment 75, 113–126.

Klemedtsson, L., Jansson, P.-E., Gustafsson, D., Karlberg, L., Weslin, P., von Arnold, K., Ernfors, M., Langvall, O., Lindroth, A., 2008. Bayesian calibration method used to elucidate carbon turnover in forest on drained organic soil. Biogeochemistry 89, 61–79.

Lawrence, D.M., Slater, A.G., 2005. A projection of severe near-surface permafrost degradation during the 21st century. Geophysical Research Letters 32. http://dx.doi.org/10.1029/2005GL025080 L24401.

Li, X., Cheng, G.D., Jin, H.J., Kang, E.S., Che, T., Jin, R., 2008. Cryospheric change in China. Global and Planetary Change 62, 210–218.

Liu, X., Chen, B., 2000. Climatic warming in the Tibetan Plateau during recent decades. International Journal of Climatology 20, 1729–1742.

Lundmark, A., 2008. Monitoring Transport and Fate of De-icing Salt in the Roadside Environment — Modelling and Field Measurements, TRITA-LWR PHD 1038, PhD thesis, KTH, Stockholm, Sweden, pp. 1–47.

Ma, Y., Su, Z., Koike, T., Yao, T., Ishikawa, H., Ueno, K., Menenti, M., 2003. On measuring and remote sensing surface energy partitioning over the Tibetan Plateau from GAME/Tibet to CAMP/Tibet. Physics and Chemistry of the Earth, Part B: Hydrology, Oceans and Atmosphere 28, 63–74.

Mellander, P.E., Laudon, H., Bishop, K., 2005. Modelling variability of snow depths and soil temperatures in Scots pine stands. Agricultural and Forest Meteorology 133, 109–118.

Mölders, N., Romanovsky, V.E., 2006. Long-term evaluation of the hydro- thermodynamic soil-vegetation scheme's frozen ground/permafrost component using observations at Barrow, Alaska. Journal of Geophysical Research 111. http://dx.doi.org/10.1029/2005JD005957 D04105.

Nelson, F.E., Anisimov, O.A., 1993. Permafrost zonation in Russia under anthropogenic climatic change. Permafrost and Periglacial Processes 4, 137–148.

Nelson, F.E., Lachenbruch, A.H., Woo, M.K., Koster, E.A., Osterkamp, T.E., Gavrilova, M.K., Cheng, G.D., 1993. Permafrost and changing climate. Proceedings of the Sixth International Conference on Permafrost, vol. 2. South China University of Technology Press, Wushan, Guangzhou, pp. 987–1005.

Nicolsky, D.J., Romanovsky, V.E., Alexeev, V.A., Lawrence, D.M., 2007. Improved modeling of permafrost dynamics in Alaska in a GCM land-surface scheme. Geophysical Research Letters 34. http://dx.doi.org/10.1029/2007GL029525 L08501.

Ohata, T., Ueno, K., Endoh, N., Zhang, Y.S., 1994. Meteorological observations in the Tanggula Mountains, Qingzang (Tibet) Plateau from 1989 to 1993. Bulletin of Glaciological Research 12, 77–86.

Osterkamp, T.E., 2007. Characteristics of the recent warming of permafrost in Alaska. Journal of Geophysical Research 112, F02S02. http://dx.doi.org/10.1029/2006JF000578.

Snow Hydrology, 1956. Summary Reports of the Snow Investigations. North Pacific Division, Corps of Engineers, U.S. Army, Portland, Oregon (437 pp.).

Stendel, M., Christensen, J.H., 2002. Impact of global warming on permafrost conditions in a coupled GCM. Geophysical Research Letter 29. http://dx.doi.org/10.1029/2001GL014345.

van Genuchten, M.Th., 1980. A closed-form equation for predicting the hydraulic conductivity of unsaturated soils. Soil Science Society of America Journal 44, 892–898.

Wang, Q.C., Li, L., Wang, Z.Y., Li, D.L., Qing, N.S., Zhu, X.D., Shi, X.H., 2005. Response of permafrost over Qinghai Plateau to climate warming. Plateau Meteorology 24, 708–713.

Wang, G.X., Li, Y.S., Hu, H.C., Wang, Y.B., 2008. Synergistic effect of vegetation and air temperature changes on soil water content in alpine frost meadow soil in the permafrost region of Qinghai–Tibet. Hydrological Processes 22, 3310–3320.

Wang, G.X., Hu, H.C., Li, T.B., 2009. The influence of freeze–thaw cycles of active soil layer on surface runoff in a permafrost watershed. Journal of Hydrology 375, 438–449.

Weller, G., Chapin, F.S., Everett, K.R., Hobbie, J.E., Kane, D., Oechel, W.C., Ping, C.L., Reeburgh, W.S., Walker, D., Walsh, J., 1995. The Arctic Flux Study: a regional view of trace gas release. Journal of Biogeography 22, 365–374.

Wu, T.H., 2005. A Study of the response of permafrost to global climate change in the Qinghai–Tibetan Plateau, Ph.D Dissertation, Cold and Arid Regions Environmental and Engineering Research Institute, Chinese Academy of Science. (in Chinese with abstract).

Wu, Q.B., Liu, Y.Z., 2004. Ground temperature monitoring and its recent change in Qinghai–Tibet Plateau. Cold Regions Science and Technology 38, 85–92.

Wu, Q.B., Zhang, T.J., 2008. Recent permafrost warming on the Qinghai–Tibetan Plateau. Journal of Geophysical Research 113. http://dx.doi.org/10.1029/2007JD009539 D13108.

Wu, Q.B., Cheng, G.D., Ma, W., Niu, F., Sun, Z.Z., 2006. Technical approaches on permafrost thermal stability for Qinghai–Tibet Railway. Geomechanics and Geoengineering 1, 119–127.

Wu, Q.B., Dong, X.F., Liu, Y.Z., Jin, H.J., 2007. Responses of permafrost on the Qinghai–Tibet Plateau, China, to climate change and engineering construction. Arctic, Antarctic, and Alpine Research 39, 682–687.

Yang, J.P., Ding, Y.J., Chen, R.S., Shen, Y.P., 2004. Permafrost change and its effect on eco-environment in the source regions of the Yangtze and Yellow Rivers. Journal of Mountain Science 22, 278–285.

Yang, M.X., Yao, T.D., Nelson, F.E., Shiklomanov, N.I., Guo, D.L., Wang, C.H., 2008. Snowcover and depth of freeze–thaw on the Tibetan Plateau: a case study from 1997–1998. Physical Geography 29, 208–221.

Yang, Y., Chen, R.S., Ji, X.B., Qing, W.W., Liu, J.F., Han, C.T., 2010. Heat and water transfer processes on alpine meadow frozen grounds of Heihe mountainous in Northwest China. Advances in Water Science 21, 30–35 (in Chinese).

Zhang, T.J., 2005. Influence of the seasonal snow cover on the ground thermal regime: an overview. Reviews of Geophysics 43. http://dx.doi.org/10.1029/2004RG000157 RG4002.

Zhang, T.J., Armstrong, R.L., 2001. Soil freeze/thaw cycles over snow-free land detected by passive microwave remote sensing. Geophysical Research Letter 28, 763–766.

Zhang, Y., Yao, T., Pu, J., 1997. The features of hydrological processes in the Dongkemadi River Basin, Tanggula Pass, Tibetan Plateau. Journal of Glaciology and Geocryology 19, 214–222.

Zhang, T.J., Barry, R.G., Gilichinsky, D., Bykhovets, S.S., Sorokovikov, V.A., Ye, J., 2001. An amplified signal of climatic change in soil temperatures during the last century at Irkutsk, Russia. Climatic Change 49, 41–76.

Zhang, T.J., Armstrong, R.L., Smith, J., 2003a. Investigation of the near-surface soil freeze–thaw cycle in the contiguous United States: algorithm development and validation. Journal of Geophysical Research 108 (D22).

Zhang, T.J., Barry, R.G., Knowles, K., Ling, F., Armstrong, R.L., 2003b. Distribution of seasonally and perennially frozen ground in the Northern Hemisphere. In: Phillips, M., Springman, S.M., Arenson, L.U. (Eds.), Proceedings of the 8th International Conference on Permafrost, Zurich, Switzerland. A.A. Balkema, Brookfield, Vt., pp. 1289–1294.

Zhang, T.J., Frauenfeld, O.W., Serreze, M.C., Etringer, A.J., Oelke, C., McCreight, J.L., Barry, R.G., Gilichinsky, D., Yang, D., Ye, H., Ling, F., Chudinova, S., 2005. Spatial and temporal variability of active layer thickness over the Russian Arctic drainage basin. Journal of Geophysical Research 110. http://dx.doi.org/10.1029/2004JD005642 D16101.

Zhao, L., Ping, C.L., Yang, D., Cheng, G., Ding, Y., Liu, S., 2004. Changes of climate and seasonally frozen ground over the past 30 years in Qinghai–Xizang (Tibetan) Plateau, China. Global and Planetary Change 43, 19–23.